

Synthesis and Photophysical Characterization of Stable Indium Bacteriochlorins

Michael Kraye,[†] Eunkyung Yang,[‡] Han-Je Kim,[†] Hooi Ling Kee,[‡] Richard M. Deans,[†] Camille E. Sluder,[†] James R. Diers,[§] Christine Kirmaier,[‡] David F. Bocian,^{*,§} Dewey Holten,^{*,‡} and Jonathan S. Lindsey^{*,†}

[†]Department of Chemistry, North Carolina State University, Raleigh, North Carolina 27695-8204, United States

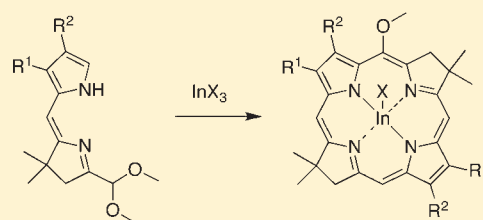
[‡]Department of Chemistry, Washington University, St. Louis, Missouri 63130-4889, United States

[§]Department of Chemistry, University of California, Riverside, California 92521-0403, United States

S Supporting Information

ABSTRACT: Bacteriochlorins have wide potential in photochemistry because of their strong absorption of near-infrared light, yet metallobacteriochlorins traditionally have been accessed with difficulty. Established acid-catalysis conditions [$\text{BF}_3 \cdot \text{OEt}_2$ in CH_3CN or $\text{TMSOTf}/2,6\text{-di-}t\text{-tert-butylpyridine}$ in CH_2Cl_2] for the self-condensation of dihydrodipyrin-acetals (bearing a geminal dimethyl group in the pyrrole ring) afford stable free base bacteriochlorins. Here, InBr_3 in CH_3CN at room temperature was found to give directly the corresponding indium bacteriochlorin. Application of the new acid catalysis conditions has

afforded four indium bacteriochlorins bearing aryl, alkyl/ester, or no substituents at the β -pyrrolic positions. The indium bacteriochlorins exhibit (i) a long-wavelength absorption band in the 741–782 nm range, which is shifted bathochromically by 22–32 nm versus the analogous free base species, (ii) fluorescence quantum yields (0.011–0.026) and average singlet lifetime (270 ps) diminished by an order of magnitude versus that (0.13–0.25; 4.0 ns) for the free base analogues, and (iii) higher average yield (0.9 versus 0.5) yet shorter average lifetime (30 vs 105 μs) of the lowest triplet excited state compared to the free base compounds. The differences in the excited-state properties of the indium chelates versus free base bacteriochlorins derive primarily from a 30-fold greater rate constant for $S_1 \rightarrow T_1$ intersystem crossing, which stems from the heavy-atom effect on spin–orbit coupling. The trends in optical properties of the indium bacteriochlorins versus free base analogues, and the effects of 5-OMe versus 5-H substituents, correlate well with frontier molecular-orbital energies and energy gaps derived from density functional theory calculations. Collectively the synthesis, photophysical properties, and electronic characteristics of the indium bacteriochlorins and free base analogues reported herein should aid in the further design of such chromophores for diverse applications.



INTRODUCTION

Bacteriochlorins are an important class of tetrapyrrolic macrocycles owing to their strong near-infrared absorption band.^{1,2} This feature makes these pigments attractive candidates for a wide variety of applications, including photodynamic therapy (PDT),^{3–12} optical imaging,^{3,13–19} flow cytometry,^{19,20} and artificial photosynthesis.^{21–23} Naturally occurring bacteriochlorins such as bacteriochlorophylls (Chart 1) provide the basis for bacterial photosynthesis.¹ Palladium-containing bacteriochlorins such as WST-9^{24,25} and WST-11,²⁶ which are derived from bacteriochlorophyll *a* (Chart 1), are particularly interesting for a number of reasons when compared to their free base analogues. First, palladium bacteriochlorins readily undergo intersystem crossing to give higher yields of the triplet excited state. Second, metallobacteriochlorins in general have a bathochromically shifted long-wavelength absorption band.² Near-infrared light absorption and high triplet excited-state yields are valuable for effective photosensitization in PDT. However, the repertoire of metallobacteriochlorins prepared to date is quite limited relative to that of metalloporphyrins and metallochlorins. The dearth stems from limitations in access to and stability of the

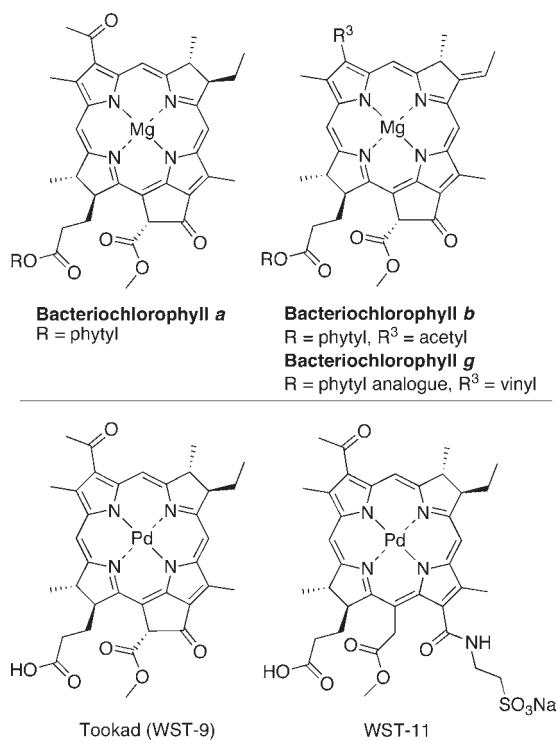
bacteriochlorin macrocycles, which serve as tetradentate ligands to the metal, as well as limitations in approaches for metalation.

The primary source of bacteriochlorins has stemmed from semisynthesis beginning with the bacterial photosynthetic pigment bacteriochlorophyll *a*.^{8,11} Two significant problems with derivatives of the bacteriochlorophylls include limited stability^{25,27} and poor synthetic malleability owing to the presence of a nearly full complement of substituents about the perimeter of the macrocycle.^{8,11} Nonetheless, macrocycles derived from bacteriochlorophylls have been metalated with a number of divalent metals (Mn^{2+} , Co^{2+} , Ni^{2+} , Cu^{2+} , Zn^{2+} , Pd^{2+} , and Cd^{2+}).² The methods for preparing such metallobacteriochlorins include conversion of the free base macrocycle to a Cd^{2+} chelate followed by transmetalation,²⁸ magnesianation of the free base macrocycle with a hindered Grignard reagent,²⁹ or, for selected derivatives, direct treatment with a metal salt.³⁰ The photodynamics of such divalent metallobacteriochlorins have been examined.³¹ On the other hand, fewer metals (Ni^{2+} , Cu^{2+} , Zn^{2+})

Received: February 16, 2011

Published: April 13, 2011

Chart 1

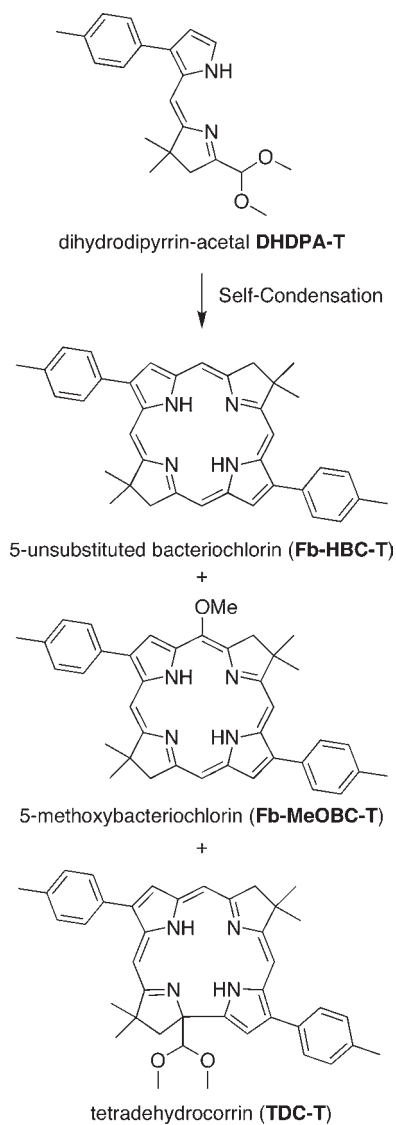


have been inserted into wholly synthetic bacteriochlorins. The set of these ligands is also very limited and includes *meso*-tetraaryl bacteriochlorins,^{32–35} 1,5-dihydroxy-1,5-dimethyloctaethylbacteriochlorin,³⁶ and 3,13-dicyano-8,8,18,18-tetramethylbacteriochlorin.³⁷ The scarcity of synthetic metallo bacteriochlorins reflects the dual problems of preparing and metalating the bacteriochlorin ligand.

Recently, we developed a concise route to stable bacteriochlorins that entails self-condensation of a dihydrodipyrin-acetal (Scheme 1).³⁸ Investigation of a wide variety of Lewis acids for the self-condensation revealed two acid conditions that give free base bacteriochlorin formation: $\text{BF}_3 \cdot \text{OEt}_2$ in CH_3CN and $\text{TMSOTf}/2,6\text{-di-}t\text{-butylpyridine}$ (2,6-DTBP) in CH_2Cl_2 .^{38,39} Use of $\text{BF}_3 \cdot \text{OEt}_2$ in CH_3CN for the *p*-tolyl-substituted dihydrodipyrin-acetal (DHDPA-T) results in a mixture of a free base 5-unsubstituted bacteriochlorin (Fb-HBC-T), a free base 5-methoxybacteriochlorin (Fb-MeOBC-T), and a free base B, D-tetradhydrocorrin (TDC-T), with Fb-HBC-T being the predominant macrocycle at the optimized conditions.³⁸ Use of $\text{TMSOTf}/2,6\text{-DTBP}$ in CH_2Cl_2 exclusively gives Fb-MeOBC-T.^{39,40} Other acids investigated resulted either in lower yields of free base bacteriochlorins, preferential formation of TDC-T, or gave no macrocycle. One exception was InCl_3 in CH_3CN , which resulted in an indium bacteriochlorin (In-MeOBC-T) along with free base Fb-MeOBC-T and TDC-T.

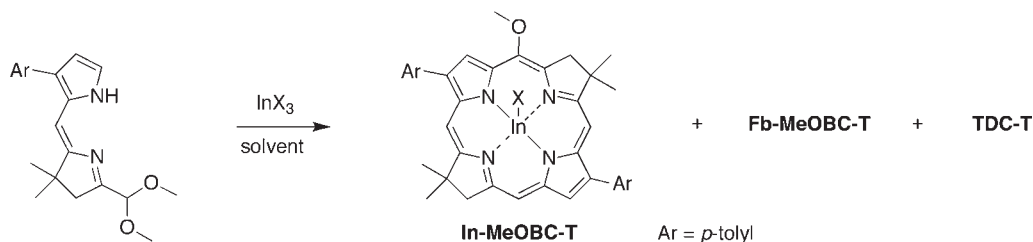
To our knowledge, no other indium bacteriochlorins have been described. An indium isobacteriochlorin has been reported by Buchler et al.⁴¹ Indium chlorins derived from natural chlorophylls have been extensively used in photodynamic therapy studies because of their high yield of the excited triplet state.⁴² The reported indium chlorins result from metalation of the corresponding free base chlorin. Indium porphyrins have also been used for PDT as well as photophysical applications,^{43–45}

Scheme 1



yet also are derived from the free base analogues (except an indium ABCD-porphyrin, which was synthesized via a bilane⁴⁶). In addition to the expected bathochromic shift of the long-wavelength absorption band and the high yield of triplet state, the presence of a tricationic metal chelate introduces a polar site at the core of the macrocycle, providing a more hydrophilic bacteriochlorin, which may be attractive for a number of photobiological studies.

Herein, we report the results of an investigation of InX_3 -mediated catalysis of the conversion of dihydrodipyrin-acetals to the corresponding metallo bacteriochlorins. The paper is divided into three parts. Part 1 concerns the identification, optimization, and scope of application of the reaction conditions for the in situ formation of indium bacteriochlorins. Part 2 provides a comprehensive study of the spectral (absorption, fluorescence) and photophysical properties of the indium bacteriochlorins. Finally, part 3 correlates the molecular orbital characteristics (energies and electron density distributions) and the photophysical properties of the bacteriochlorins owing to the metalation state

Table 1. Self-Condensation of DHDPA-T Using InX_3 ^a

entry	InX_3 /solvent	In-MeOBC-T % yield	Fb-MeOBC-T % yield	Fb-HBC-T % yield	TDC-T % yield
1	$\text{In}(\text{OTf})_3/\text{CH}_2\text{Cl}_2$	<i>b</i>	11.1	9.4	observed ^c
2	$\text{In}(\text{OTf})_3/\text{CH}_3\text{CN}$	<i>b</i>	14.3	trace	observed ^c
3	$\text{InCl}_3/\text{CH}_2\text{Cl}_2$	<i>b</i>	<i>b</i>	0.64	observed ^c
4	$\text{InCl}_3/\text{CH}_3\text{CN}$	4.5	<i>b</i>	<i>b</i>	<i>b</i>
5	$\text{InBr}_3/\text{CH}_2\text{Cl}_2$	<i>b</i>	<i>b</i>	<i>b</i>	<i>b</i>
6	$\text{InBr}_3/\text{CH}_3\text{CN}$	9.5	<i>b</i>	<i>b</i>	<i>b</i>

^a All reactions were carried out (4-mL scale) with 5 mM DHDPA-T and an amount of InX_3 corresponding to 50 mM (regardless of solubility) at room temperature. Each reaction was carried out for 16 h. ^b Not detected. ^c Observed by TLC but not isolated.

(indium versus free base) and substituents at the perimeter of the macrocycle.

RESULTS AND DISCUSSION

1. In situ Synthesis of Indium Bacteriochlorins. *A. Examination of Conditions.* The self-condensation of DHDPA-T was examined at room temperature using an indium catalyst [InCl_3 , InBr_3 , or $\text{In}(\text{OTf})_3$] in CH_3CN or CH_2Cl_2 . The reactions were conducted with 5 mM DHDPA-T (0.02 mmol scale) and 50 mM InX_3 . Each reaction mixture was stirred for 16 h at room temperature, at which point those reactions that showed traces of bacteriochlorin in the crude reaction mixture by UV-vis spectroscopy [$Q_y(0,0)$ absorption band >700 nm] were quenched by the addition of triethylamine. Bacteriochlorins were isolated by chromatography, whereupon yields were determined spectroscopically. The results are summarized in Table 1. $\text{In}(\text{OTf})_3$ gave only the free base bacteriochlorins (entries 1 and 2). Use of InCl_3 or InBr_3 in CH_2Cl_2 gave no indium bacteriochlorin (entries 3 and 5); however, InCl_3 or InBr_3 in CH_3CN gave In-MeOBC-T in 4.5% or 9.5% yield, respectively (entries 4 and 6). The self-condensation of DHDPA-T upon treatment with InCl_3 in CHCl_3 , 1,2-dichloroethane, tetrahydrofuran (THF), methanol, ethanol, pyridine, dimethylformamide (DMF), or dimethyl sulfoxide (DMSO) resulted in substantially lower yield or no bacteriochlorin (see Supporting Information, Table S1).

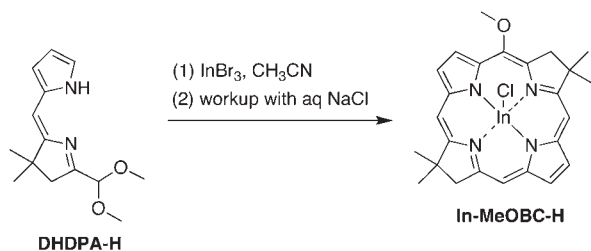
As part of a study of the condensation conditions, the following observations were made:

- (i) A 4×4 factorial design spanning concentrations of DHDPA-T (5–20 mM) and InBr_3 (25–100 mM) in CH_3CN was conducted on a small scale (see Supporting Information, Table S2). The best conditions (13 mM DHDPA-T and 40 mM InBr_3) thereby identified were applied at larger scale (1.48 mmol of DHDPA-T), which afforded Fb-MeOBC-T, TDC-T, and In-MeOBC-T in yield of 1.8%, 3.7%, and 14.6%, respectively.
- (ii) The reaction with InBr_3 in CH_3CN was homogeneous whereas that with InCl_3 was heterogeneous given the

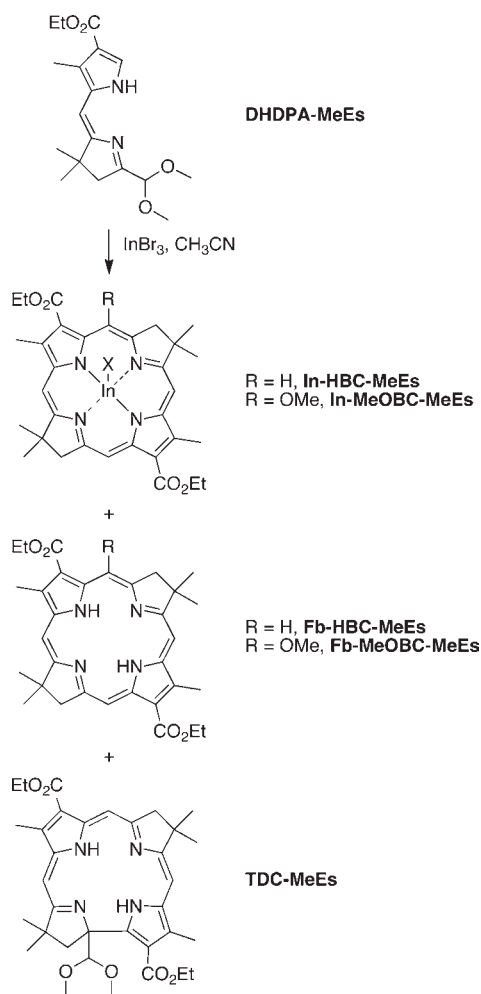
respective solubility limits of the two acids (>650 mM versus 5–10 mM). Treatment of DHDPA-T with a homogeneous saturated solution of InCl_3 in CH_3CN gave In-MeOBC-T in 4% yield versus 8% upon reaction in a suspension of InCl_3 (see Supporting Information).

- (iii) Inclusion of an InX_3 species with the known acid-catalysis conditions for conversion of DHDPA-T to the corresponding bacteriochlorins did not afford any synergy in yield. The optimized conditions include 5 mM DHDPA-T and 50 mM $\text{BF}_3 \cdot \text{OEt}_2$ in CH_3CN for formation of Fb-HBC-T; and 18 mM DHDPA-T, 72 mM TMSOTf, and 144 mM 2,6-DTBP in CH_2Cl_2 for formation of Fb-MeOBC-T (see Supporting Information).
- (iv) Treatment of a 5 mM solution of Fb-MeOBC-T in CH_3CN with 5 equiv (25 mM) of InCl_3 or InBr_3 did not result in any indium bacteriochlorin. However, treatment of a 5 mM solution of Fb-MeOBC-T in CH_3CN with 50 equiv of InBr_3 (250 mM) gave In-MeOBC-T in 14% yield, with recovery of a significant amount (57% yield) of unreacted free base bacteriochlorin (Fb-MeOBC-T). The absence of direct insertion of indium into the free base bacteriochlorin under conditions closely mimicking those of the dihydropyrrin-acetal self-condensation argues against metalation after macrocycle formation, and thus is consistent with a mechanism wherein metalation occurs during the course of a templating process.
- (v) Other group III metals were investigated. Examination of GaCl_3 or GaBr_3 in CH_3CN for the self-condensation of DHDPA-T gave no metallo bacteriochlorin and only trace amounts (<1%) of free base bacteriochlorin, respectively. Aluminum-based Lewis acids such as AlMe_3 , AlCl_3 or $\text{Al}(\text{acac})_3$ examined previously gave low or no yields of free base bacteriochlorin.³⁹ Thallium reagents were not investigated owing to toxicity concerns. In summary, the self-condensation of DHDPA-T with $\text{BF}_3 \cdot \text{OEt}_2$ gives free base bacteriochlorins Fb-MeOBC-T and Fb-HBC-T, whereas InCl_3 and InBr_3 give indium bacteriochlorin In-MeOBC-T.

Scheme 2



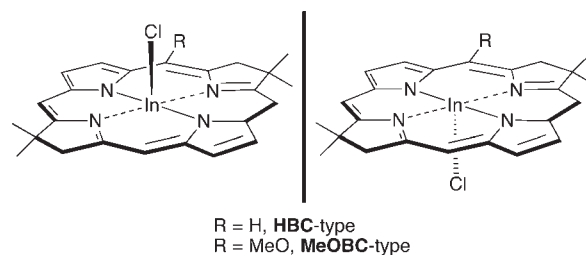
Scheme 3



B. Scope of Reaction. Extension of the best conditions ($\text{InBr}_3/\text{CH}_3\text{CN}$) to the unsubstituted dihydropyrrin-acetal **DHDPA-H** resulted in indium 5-methoxybacteriochlorin **In-MeOBC-H** in 8.6% yield after column chromatography (Scheme 2). Neither free base bacteriochlorin nor **TDC**-type macrocycles were observed. **In-MeOBC-H** showed absorption at 740 nm (compared to 709 nm of the free base analogue) and a molecular ion peak at $m/z = 513$. However, a ^1H NMR spectrum of satisfactory quality could not be obtained for **In-MeOBC-H**.

Treatment of the methyl/ester-substituted dihydropyrrin-acetal **DHDPA-MeEs** with InBr_3 in CH_3CN resulted in a

Chart 2



mixture of free base and indium bacteriochlorins (both 5-methoxy and 5-unsubstituted), along with the tetradehydrocorrins **TDC-MeEs** (Scheme 3). The yields of **Fb-HBC-MeEs** (2.4%, 11 mg), **Fb-MeOBC-MeEs** (1.6%, 7.7 mg), **TDC-MeEs** (11.1%, 55 mg), **In-HBC-MeEs** (1.0%, 5.5 mg), and **In-MeOBC-MeEs** (1.7%, 10.9 mg) were quite low. Optimization of the condensation conditions for **DHDPA-MeEs** lies beyond the scope of the present study. Nevertheless, the macrocycles obtained were readily isolated in sufficient quantities for spectroscopic characterization. **Fb-MeOBC-MeEs** has been previously reported³⁹ whereas **Fb-HBC-MeEs**, **In-HBC-MeEs**, **In-MeOBC-MeEs**, and **TDC-MeEs** are new compounds and were fully characterized herein.

C. Molecular Characterization. The LD-MS spectrum of **In-MeOBC-T** gave the molecular ion peak ($m/z = 727.9$), which is consistent with the molecular formula $\text{C}_{39}\text{H}_{38}\text{ClInN}_4\text{O}$ (calcd 728.1773), and a peak attributed to the indium bacteriochlorin with loss of chloride ($m/z = 692.8$). For all other indium bacteriochlorins described herein the mass spectrometry data (ESI-MS or LD-MS) only gave peaks consistent with loss of the counterion. Although the use of InBr_3 is expected to initially afford the bromide counterion, in each case the reaction mixture was worked up by washing with saturated aqueous NaCl with the aim of exchanging the apical ligand with chloride. In this regard, indium porphyrins readily undergo ligand exchange.^{47,48} Each indium bacteriochlorin was purified by silica gel column chromatography. The indium bacteriochlorins were more polar and eluted more slowly than the free base analogues. The slow chromatographic elution may stem from an equilibrium between associated and dissociated forms of the complex (consisting of the indium bacteriochlorin and the apical counterion). Nonetheless, elemental analysis of **In-MeOBC-T** revealed the presence of chloride with no detectable bromide, whereas elemental analysis of **In-MeOBC-T** revealed the presence of chloride with a trace (<2.5%) of bromide. Consequently, the apical ligand is assumed to be chloride for all yield calculations.

Indium porphyrins (e.g., $\text{In}(\text{TPP})(\text{OAc})$) are square-pyramidal with the indium displaced ~ 0.7 Å from the plane of the macrocycle.⁴⁹ For the indium bacteriochlorins (**In-MeOBC-H**, **In-MeOBC-T**, **In-MeOBC-MeEs**, and **In-HBC-MeEs**), the presence of the In-X group on one face or the other of the macrocycle results in a mixture of enantiomers as illustrated in Chart 2, and a different magnetic environment for those protons that project out of the plane on one side or the other of the macrocycle. The presence of the 5-methoxy group further reduces the symmetry from C_2 (e.g., **In-HBC-MeEs**) to C_1 (e.g., **In-MeOBC-MeEs**), causing the two pyrrolic (or pyrrolinyl) rings to be in different magnetic environments.

The NMR data are consistent with an out-of-plane geometry, which causes the two faces of the macrocycle to be diastereotopic.

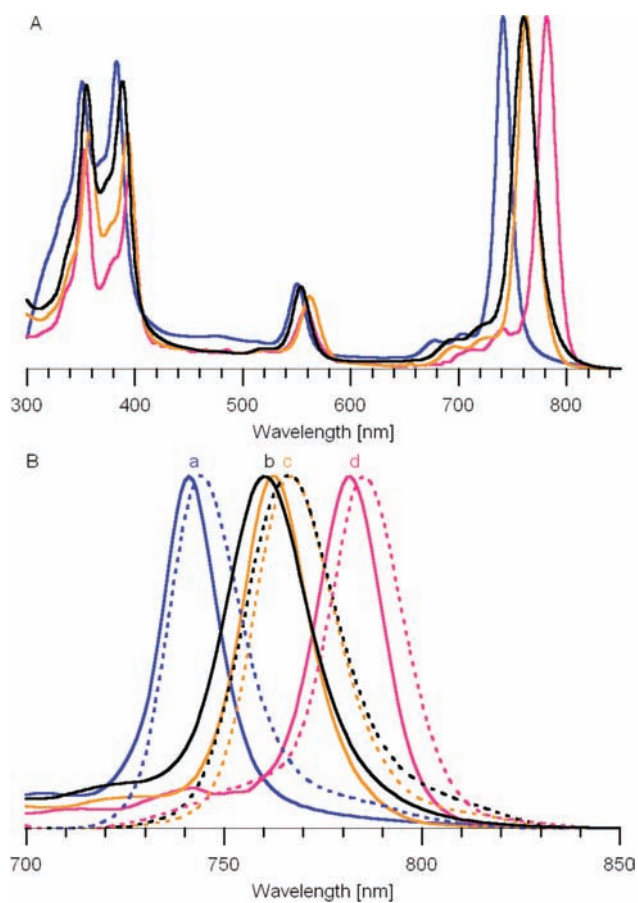
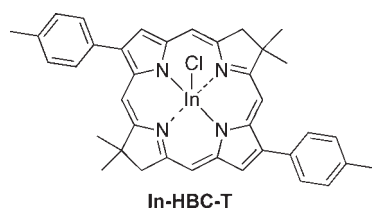


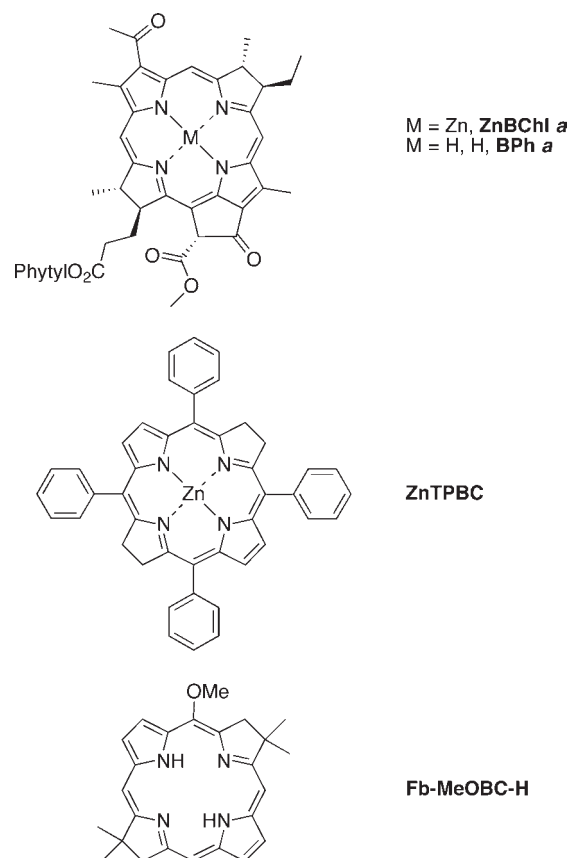
Figure 1. Spectra in toluene at room temperature of indium bacteriochlorins (normalized at the Q_y bands). (A) Absorption spectra. (B) Magnification of Q_y region showing absorption (solid lines) and emission (dashed lines) spectra. The labels and the colors are as follows: **In-MeOBC-H** (a, blue), **In-MeOBC-T** (b, black), **In-MeOBC-MeEs** (c, orange), **In-HBC-MeEs** (d, magenta).

Chart 3



Thus, in bacteriochlorin **In-MeOBC-T**, with C_1 symmetry, the two geminal dimethyl groups give rise to four singlets (δ 1.80, 1.81, 2.05, and 2.08 ppm), and the CH_2 group in each of the reduced pyrrole rings gives rise to a pair of doublets ($J = 17.2$ or 17.8 Hz) in the region of δ 4.36–4.61 ppm. The methoxy group resonates as a singlet downfield (δ 4.52), the aryl protons of each *p*-tolyl group give a pair of doublets (δ 7.56–7.58 ppm and 8.01–8.06 ppm), and each of the five peripheral protons (3, 10, 13, 15, and 20 positions) gives rise to an apparent singlet (δ 8.66, 8.71, 8.75, 8.78, and 8.99 ppm). The indium bacteriochlorins failed to give good quality ^{13}C NMR spectra. Furthermore, **In-MeOBC-H** did not give a quality ^1H NMR spectrum (vide supra).

Chart 4



2. Spectral and Photophysical Properties. *A. Absorption Spectra.* The ground state electronic absorption spectra of the four indium bacteriochlorins **In-MeOBC-H**, **In-MeOBC-T**, **In-MeOBC-MeEs**, and **In-HBC-MeEs** in toluene are shown in Figure 1 (solid lines). The spectral data for these four indium bacteriochlorins, and for **In-HBC-T** (Chart 3; Fan, D.; Lindsey, J. S. unpublished data), are listed in Table 2. For comparison, Table 2 also lists spectral data for the base analogues **Fb-MeOBC-H** (Chart 4); **Fb-MeOBC-T** (Scheme 1); **Fb-MeOBC-MeEs** and **Fb-HBC-MeEs** (Scheme 3); and **Fb-HBC-T** (Scheme 1).^{38,39} The table also includes spectral data for two literature reference compounds, zinc *meso*-tetraphenylbacteriochlorin (**ZnTPBC**)^{33,35} and zinc bacteriochlorophyll *a* (**ZnBChl a**)²⁸ as well as the two naturally occurring pigments, bacteriochlorophyll *a* (**BChl a**)¹ and bacteriopheophytin *a* (**BPh a**)¹ (Charts 1 and 4).

The absorption spectrum of each bacteriochlorin contains four main features with maxima generally in the following spectral ranges: $B_y(0,0)$ (350–360 nm), $B_x(0,0)$ (365–395 nm), $Q_x(0,0)$ (495–570 nm), and $Q_y(0,0)$ (700–800 nm). Each of these four origin transitions has a weaker (1,0) vibronic satellite feature roughly 1250 cm^{-1} to higher energy. [Note that the B_x and B_y transitions may have mixed x and y polarization and for some compounds are spectrally overlapped.] The absorption spectrum of **In-MeOBC-T** (355, 388, 553, 760 nm) in toluene is quite similar to that of **ZnTPBC** (350, 385, 540, and 760 nm)³⁵ in CH_2Cl_2 , and of **ZnBChl a** (353, 389, 558, and 762 nm)²⁸ in diethyl ether (Table 2).

The $Q_y(0,0)$ transition is of particular interest because it corresponds to absorption of light to produce the lowest singlet

Table 2. Spectral Characteristics of Indium, Free Base, and Reference Bacteriochlorins^a

compound	B _y (0,0) ^b abs (nm)	B _x (0,0) ^b abs (nm)	Q _x (0,0) abs (nm)	Q _y (0,0) ^c abs (nm)	Q _y ^d abs fwhm (nm)	Q _y (0,0) ^e em (nm)	Q _y ^f em fwhm (nm)	ΔQ _y ^g abs-em (cm ⁻¹)	I _{Q_y} / I _B ^h	ΣQ _y / ΣB ⁱ
<i>Indium Bacteriochlorins</i>										
In-MeOBC-H	352	384	552	741 [+32]	19	747	24	108	1.1	0.13
In-MeOBC-T	355	388	553	760 [+29]	23	767	30	120	0.91	0.14
In-HBC-T	350	388	539	763 [+27]	23	769	31	102	1.1	0.15
In-MeOBC-MeEs	358	393	563	762 [+24]	20	768	27	103	1.6	0.23
In-HBC-MeEs	354	395	559	782 [+22]	21	785	23	49	1.3	0.17
<i>Free Base Bacteriochlorins</i>										
Fb-MeOBC-H	354	367	501	709	11	711	18	40	0.87	0.11
Fb-MeOBC-T	356	380	511	731	20	736	23	93	0.89	0.14
Fb-HBC-T	351	374	499	736	20	742	23	110	1.0	0.14
Fb-MeOBC-MeEs	357	398	520	738	18	741	21	217	0.96	0.13
Fb-HBC-MeEs	354	384	520	760	18	764	20	69	0.98	0.19
<i>Reference Bacteriochlorins</i>										
ZnTPBC ^j	350	385	540	760						
ZnBChl ^k	353	389	558	762						
BChl ^l	363	396	581	781	32	789	29	130	1.39	0.23
BPh ^a	362	389	532	758	31	768	27	172	0.69	0.15

^a Obtained in toluene at room temperature. ^b The two Soret features are labeled B_x(0,0) and B_y(0,0) but the bands may be of mixed parentage. ^c Position (nm) of the Q_y(0,0) absorption band. The value in brackets is the difference in wavelength of the Q_y(0,0) band of the indium bacteriochlorin versus the free base analogue. ^d Full-width-at-half-maximum (fwhm in nm) of the Q_y(0,0) absorption band. ^e Position (nm) of the Q_y(0,0) fluorescence emission band. ^f fwhm of the Q_y(0,0) fluorescence band. ^g Difference in energy (cm⁻¹) between the peak positions of the Q_y(0,0) absorption and fluorescence bands. ^h Ratio of the peak intensities of the Q_y(0,0) band to the Soret (B) maximum, which could be either B_x(0,0) or B_y(0,0). ⁱ Ratio of the integrated intensities of the Q_y manifold [Q_y(0,0), Q_y(1,0)] to the Soret manifold [B_y(0,0), B_y(1,0), B_x(0,0), B_x(1,0)], for spectra plotted in cm⁻¹. ^j Reference 35 in CH₂Cl₂. ^k Reference 28 in diethyl ether. ^l In benzene.

excited state, which dominates much of the photophysical behavior. The Q_y(0,0) band for the five indium bacteriochlorins is positioned on the average 27 nm (22–32 nm) to longer wavelength than those for the free base analogues. Similarly, the Q_x(0,0) band for the indium chelates lies on the average 43 nm (39–51 nm) to longer wavelength than those for the free base compounds (Table 2). The average value of the full-width-at-half-maximum (fwhm) of the Q_y(0,0) absorption band of the indium bacteriochlorins is 21 nm, which is only slightly greater than the value of 17 nm for the free base analogues.

B. Fluorescence Spectra. The fluorescence emission spectra of the four indium bacteriochlorins **In-MeOBC-H**, **In-MeOBC-T**, **In-MeOBC-MeEs**, and **In-HBC-MeEs** in toluene are shown in Figure 1 (dashed lines). The emission spectral characteristics for these four compounds, **In-HBC-T**, the free base analogues, and several synthetic reference and naturally occurring bacteriochlorins are listed in Table 2. The fluorescence spectrum of each bacteriochlorin is dominated by the Q_y(0,0) band. The spectra shown in Figure 1 reveal very weak features ~25 nm to shorter wavelength than the Q_y(0,0) fluorescence band of the indium bacteriochlorins. These weak, higher-energy features are at the positions expected for the free base analogues. Weak emission from the free base is visible even when present in trace amounts because the free base bacteriochlorin has a fluorescence quantum yield roughly an order of magnitude greater than that for the indium chelate (see below).

The Q_y(0,0) fluorescence maximum of the indium bacteriochlorins lies on the average 6 nm to longer wavelength (96 cm⁻¹ to lower energy) than the Q_y(0,0) absorption maximum (Table 2). A similar small “Stokes” shift is generally observed for the free

base bacteriochlorins. The average bandwidth (fwhm) of the Q_y(0,0) fluorescence feature of the indium bacteriochlorins is 27 nm, which is about 25% larger than the value of 21 nm observed for the Q_y(0,0) absorption band. The Q_y(0,0) emission feature of the free base analogues is similarly larger than that of the absorption band (21 versus 17 nm).

C. Fluorescence Quantum Yields. The fluorescence quantum yields (Φ_f) of the five indium bacteriochlorins are in the range 0.011–0.026 with an average value of 0.018. The Φ_f values for the free base species are in the range 0.13–0.25 with an average of 0.19. Thus, the fluorescence yields for the indium bacteriochlorins are on the average 10-fold lower than those for the free base analogues (Table 3). The data can be compared with those of **Bchl a** and **Bph a**.^{50,51}

D. Singlet Excited-State Lifetimes. The lifetime of the lowest singlet excited state (τ_S) of each indium bacteriochlorin was determined using ultrafast transient absorption spectroscopy and found to be in the range 210–330 ps with an average value of 270 ps (Table 3). The τ_S values for the free base bacteriochlorins were measured using time-resolved fluorescence spectroscopy and found to be in the range 3.0–5.0 ns with an average value of 4.0 ns (Table 3). Thus, the singlet excited-state lifetimes of the indium bacteriochlorins are about 20-fold shorter than those for the free base analogues.

E. Triplet Excited-State Lifetimes. The lifetime of the lowest triplet excited state (τ_T) of each indium and free base bacteriochlorin was measured at room temperature using transient absorption spectroscopy. The τ_T values for the indium bacteriochlorins were found to be in the range 25–44 μs with an average value of 30 μs. The triplet excited-state lifetime for each indium

Table 3. Photophysical and Molecular Orbital Properties of Indium, Free Base, and Reference Bacteriochlorins^a

compound	$Q_y(0,0)$ ^b energy (eV)	τ_S ^c (ns)	Φ_f ^d	Φ_{isc} ^e	τ_T ^f (μ s)	HOMO (eV)	LUMO (eV)	LUMO – HOMO (eV)
<i>Indium Bacteriochlorins</i>								
In-MeOBC-H	1.67	0.33	0.011	0.9	40	-4.62	-2.56	2.06
In-MeOBC-T	1.63	0.26	0.020	0.9	32	-4.54	-2.53	2.01
In-HBC-T	1.62	0.21	0.016	0.9	44	-4.52	-2.52	2.00
In-MeOBC-MeEs	1.63	0.32	0.026	0.9	25	-4.84	-2.85	1.99
In-HBC-MeEs	1.59	0.25	0.015	0.9	30	-4.74	-2.82	1.92
In-BC average	1.63	0.27	0.018	0.9	30	-4.65	-2.66	2.00
<i>Free Base Bacteriochlorins</i>								
Fb-MeOBC-H	1.75	5.0	0.25	0.55	107	-4.48	-2.20	2.28
Fb-MeOBC-T	1.70	4.5	0.20	0.42	107	-4.42	-2.23	2.19
Fb-HBC-T	1.68	3.3	0.18	0.55	163	-4.40	-2.22	2.18
Fb-MeOBC-MeEs	1.68	4.4	0.17	0.53	85	-4.61	-2.45	2.16
Fb-HBC-MeEs	1.63	3.0	0.13	0.52	64	-4.67	-2.57	2.10
Fb-BC average	1.69	4.0	0.19	0.51	105	-4.52	-2.34	2.18
<i>Reference Bacteriochlorins</i>								
BChl <i>a</i> ^g	1.59	3.1	0.12	0.33	52	-4.75	-2.86	1.89
BPh <i>a</i> ^h	1.64	2.7	0.10	0.54	25	-4.87	-2.84	2.03

^a Obtained in toluene at room temperature unless noted otherwise. The molecular orbital energies were obtained from DFT calculations. ^b Energy of the $Q_y(0,0)$ absorption band (see Table 2). ^c Lifetime of the lowest singlet excited state measured via transient absorption spectroscopy for indium bacteriochlorins (± 20 ps) and by fluorescence techniques for the free base bacteriochlorins ($\pm 5\%$). ^d Fluorescence quantum yield $\pm 15\%$ for the indium bacteriochlorins and $\pm 5\%$ for the free base bacteriochlorins. ^e Yield of the lowest triplet excited state measured via transient absorption spectroscopy (± 0.1 for indium bacteriochlorins and ± 0.08 for the free base bacteriochlorins). ^f Lifetime of the lowest triplet excited state measured via transient absorption spectroscopy for compounds in Ar-purged 2-methyltetrahydrofuran ($\pm 10\%$). ^g The absorption and emission spectral properties, Φ_f and τ_S were acquired here in benzene and τ_T in pyridine. The value of $\Phi_T = 0.32$ was measured in toluene. Values of 0.44 and 0.41 were measured in acetonitrile and pyridine, respectively. Values of $\Phi_T = 0.32$ and $\tau_T \sim 60 \mu$ s (mixed first and second order decay) have been reported and are the average of values measured in acetonitrile, dimethylsulfoxide and pyridine.⁵⁰ ^h The values found here in ethanol are $\Phi_f = 0.081$, $\tau_S = 2.3$ ns, and $\tau_T = 30 \mu$ s. The values in acetone/methanol (7:3) are $\tau_S = 2.0$ ns, $\tau_S = 16 \mu$ s, and $\Phi_{isc} = 0.57$ (average of 0.54 and 0.60 from two methods).⁵¹

chelate is shorter than that for the free base bacteriochlorin, which were found to be in the range 64–163 μ s with an average value of 105 μ s (Table 3).

F. Triplet Excited-State Quantum Yields. The quantum yield of intersystem crossing from the lowest singlet excited state to the lowest triplet excited state (Φ_{isc}), also known as the triplet yield, was determined using transient absorption spectroscopy.⁴⁴ The Φ_{isc} values for the indium chelates were found to be 0.9 ± 0.1 . These values are considerably greater than those for the free base analogues, which were found to lie in the range 0.42–0.55 (± 0.08) with an average value of 0.51.

G. Excited-State Decay Pathways and Rate Constants. The observables τ_S , Φ_f and Φ_{isc} (Table 3) for decay of the lowest-energy singlet excited state (S_1) are connected to the rate constants for $S_1 \rightarrow S_0$ spontaneous fluorescence (k_f), $S_1 \rightarrow S_0$ internal conversion (k_{ic}), and $S_1 \rightarrow T_1$ intersystem crossing (k_{isc}) via eqs 1 to 3.

$$\tau_S = (k_f + k_{ic} + k_{isc})^{-1} \quad (1)$$

$$\Phi_f = k_f / (k_f + k_{ic} + k_{isc}) \quad (2)$$

$$\Phi_{isc} = k_{isc} / (k_f + k_{ic} + k_{isc}) \quad (3)$$

The internal conversion yield can be calculated from eq 4.

$$\Phi_{ic} = 1 - \Phi_f - \Phi_{isc} \quad (4)$$

The radiative, intersystem-crossing, and internal-conversion rate constants can be calculated from the above quantities via eq 5, where

$i = f, isc, \text{ or } ic.$

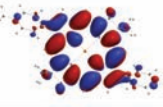
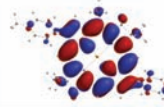
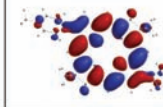
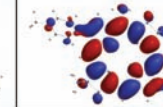
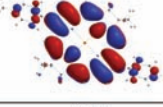
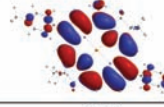
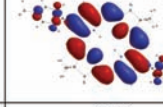
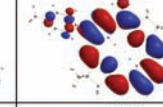
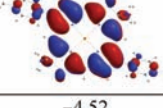
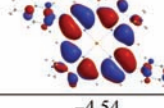
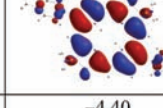
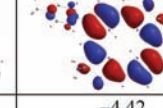
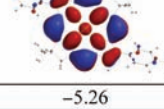
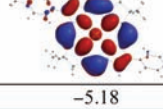
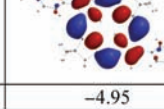
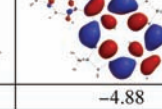
$$k_i = \Phi_i / \tau_S \quad (5)$$

The average radiative rate constant of $k_f = (17 \text{ ns})^{-1}$ for the indium bacteriochlorins is slightly greater than that of $(22 \text{ ns})^{-1}$ for the free base analogue, indicating a comparable or slightly higher fluorescence probability. Nevertheless, the average fluorescence yield is about 10-fold smaller for indium versus free base bacteriochlorins (0.018 versus 0.19) because of enhanced rate constants for the two nonradiative processes (internal conversion and intersystem crossing) in the indium chelates, as described below.

The average yields of $S_1 \rightarrow T_1$ intersystem crossing of 0.9 for indium bacteriochlorins and 0.51 ns for the free base analogues, together with the average S_1 lifetimes of 0.27 and 4.0 ns, respectively, translate via eq 5 into average intersystem-crossing rate constant of $k_{isc} = (0.3 \text{ ns})^{-1}$ for the indium bacteriochlorins being roughly 25-fold greater than that of $(8 \text{ ns})^{-1}$ for the free base analogues. This substantial difference in rates lie well outside the error limits largely associated with the determination of the individual intersystem-crossing yields. The enhancement in k_{isc} for indium versus free base bacteriochlorins almost certainly derives from the effect of the heavy indium ion on spin-orbit coupling, which drives the spin flips underlying the intersystem-crossing process.

The yields of $S_1 \rightarrow S_0$ internal conversion calculated via eq 4 for the five indium bacteriochlorins (0.09, 0.08, 0.08, 0.07, 0.09) have an average value of $\Phi_{ic} = 0.08$ that is about 25% of that of

Table 4. Molecular-Orbital Characteristics of Indium and Free Base Bacteriochlorins^a

Molecule	In-HBC-T	In-MeOBC-T	Fb-HBC-T	Fb-MeOBC-T
LUMO+1				
	-1.07	-1.07	-0.96	-0.96
LUMO				
	-2.52	-2.53	-2.22	-2.23
HOMO				
	-4.52	-4.54	-4.40	-4.42
HOMO-1				
	-5.26	-5.18	-4.95	-4.88

^a Obtained from DFT calculations.

$\Phi_{ic} = 0.3$ derived from the individual values for the five free base bacteriochlorins (0.2, 0.4, 0.3, 0.3, 0.4). These average yields give rise to a typical rate constant of $k_{ic} = (3 \text{ ns})^{-1}$ for the indium bacteriochlorins and $(14 \text{ ns})^{-1}$ for the free base analogues. A somewhat greater k_{isc} for indium versus free base bacteriochlorins can be rationalized for two reasons. First, on the basis of the energy-law for nonradiative decay,⁵² k_{ic} is expected to be somewhat greater for the indium versus free base bacteriochlorins because the average energy of the S_1 excited state of the indium bacteriochlorins (13086 cm^{-1} , 1.62 eV) is lower than that for the free base analogues (13543 cm^{-1} , 1.68 eV) (Table 3). Second, greater k_{ic} values for indium versus free base bacteriochlorins also may result from an improved Franck–Condon factor derived from nuclear-coordinate displacements involving the central In^{3+} ion, the apical counterion, and solvent interactions in the S_1 versus S_0 states. Such coordinate displacements should be enhanced because the In^{3+} ion and the apical counterion are displaced toward one side of the bacteriochlorin framework, which itself should be distorted from planarity. Nonplanar macrocycle distortions in tetrapyrrole complexes are thought to open up additional channels for conformational excursions (particularly in the excited state), which enhance internal conversion.⁵³

3. Correlation of Photophysical and Molecular Orbital Characteristics. *A. Molecular Orbitals.* To gain insights into the trends in the photophysical properties of the bacteriochlorins as a function of molecular characteristics, density functional theory (DFT) calculations were performed. These calculations provide the energies and electron-density distributions of the frontier molecular orbitals. The principal orbitals of interest are the highest occupied molecular orbital (HOMO), the lowest unoccupied molecular orbital (LUMO), and the HOMO-1 and LUMO+1. Table 4 gives electron density plots (and energies) for these four orbitals for two representative indium bacteriochlorins (**In-HBC-T** and **In-MeOBC-T**) and the free base analogues (**Fb-HBC-T** and **Fb-MeOBC-T**).

Attention is focused on the HOMO and LUMO, for which the individual energies and energy gap are listed in Table 3. In the following subsections, these orbital characteristics are correlated

with the wavelength (energy) of the $Q_y(0,0)$ absorption band of the indium and free base bacteriochlorins, the wavelength (energy) of the $Q_y(0,0)$ absorption band of bacteriochlorins containing a 5-OMe versus 5-H substituent, and the anticipated redox properties of the molecules.

B. Absorption Spectra of Indium versus Free Base Bacteriochlorins. The one-electron configuration resulting from light-induced promotion of an electron from the HOMO to the LUMO normally makes a significant contribution to the electronic characteristics of the lowest singlet excited state of most molecules. Thus, for a series of related tetrapyrroles, the LUMO – HOMO energy gap may be expected to reasonably track the energy of the $S_0 \rightarrow S_1$ electronic transition, namely, the $Q_y(0,0)$ band. This behavior is expected for bacteriochlorins because the wave function of the S_1 excited state is expected to be comprised of roughly 70–75% of the HOMO \rightarrow LUMO one-electron configuration, with the remainder due to the HOMO-1 \rightarrow LUMO+1 configuration.^{54–56} For example, time-dependent DFT calculations on **Fb-MeOBC-H** give percentages of 71% and 28%, respectively.

Figure 2 plots the LUMO – HOMO energy versus the energy (and wavelength) of the $Q_y(0,0)$ band for the indium bacteriochlorins and free base analogues. Both sets of molecules show good correlations, with similar slopes of the trend lines. It is expected that the trend lines for the indium and free base bacteriochlorins would be displaced along the transition-energy (horizontal) axis because the $Q_y(0,0)$ band for each indium bacteriochlorin is bathochromically shifted from the position for the free base species (Table 2). The displacement between the two sets of data and trend lines along the LUMO – LUMO (vertical) axis can be related to the formation of the indium(III) chelate from the free base analogue. These differential effects include (1) the positions of greater electron density from the metal ion (Table 3) and (2) structural changes in the macrocycle, including a distortion from planarity.

As noted above, the $Q_y(0,0)$ bands of the indium bacteriochlorins are positioned on the average 27 nm (0.06 eV) to

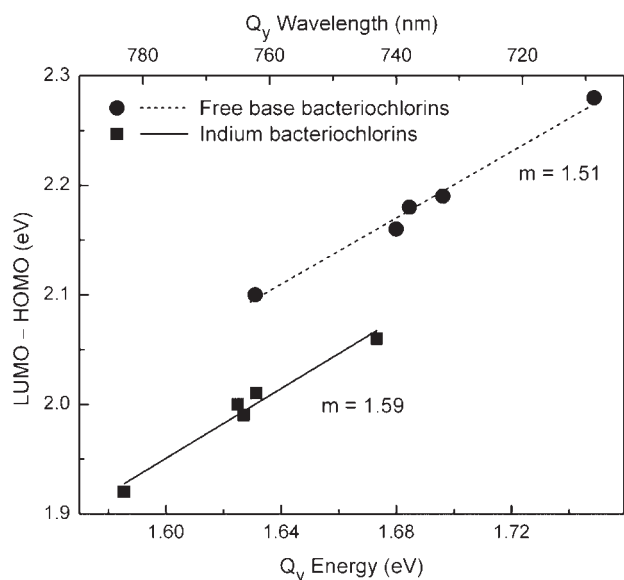


Figure 2. LUMO – HOMO energy gap versus the energy (and wavelength) of the $Q_y(0,0)$ absorption band for indium bacteriochlorins (squares and solid line) and free base bacteriochlorins (circles and dashed line). The slopes (m) of the trend lines are shown.

longer wavelength (lower energy) than those of the free base species. The indium bacteriochlorins have an average HOMO energy 0.13 eV more negative than the free base form (-4.65 vs -4.52 eV) and an average LUMO energy 0.32 eV more negative than the free base form (-2.66 vs -2.34 eV) resulting in a smaller LUMO – HOMO energy gap (2.00 vs 2.18 eV). These comparisons show that the smaller LUMO – HOMO gap and thus, the bathochromic shift in the Q_y band, derive from a more substantial metal-derived effect on the LUMO than the HOMO.

C. Effects of a 5-OMe Group on Absorption Spectra. The MO energies from the DFT calculations also track the effects of the 5-OMe versus 5-H substituent on the electronic spectra of various bacteriochlorins. For each pair of bacteriochlorins, the 5-OMe group results in a shift of the $Q_y(0,0)$ band to higher energy (shorter wavelength). The pairwise comparisons for the 5-MeO versus 5-H bacteriochlorins (Q_y energy shift, LUMO – HOMO energy-gap shift) are as follows: **In-MeOBC-T** versus **In-HBC-T** (0.01 eV, 0.01 eV); **Fb-MeOBC-T** versus **Fb-HBC-T** (0.02 eV, 0.01 eV); **In-MeOBC-MeEs** versus **In-HBC-MeEs** (0.04 eV, 0.07 eV); **Fb-MeOBC-T** versus **Fb-HBC-T** (0.05 eV, 0.06 eV). Thus, the calculations reproduce the small (0.01–0.02 eV; 3–5 nm) effect of the methoxy group for indium and free base bacteriochlorins containing 2,12-di-*p*-tolyl groups, and the larger (0.04–0.05 eV; 10–13 nm) effect of the methoxy group for indium and free base bacteriochlorins containing 2,12-dimethyl and 3,13-diester groups. Close examination of the HOMO and LUMO energies indicates that the greater effect on the -MeEs versus -T complexes is associated with a greater effect of the 5-OMe group on the HOMO than the LUMO for the indium chelates and the opposite effect for the free base compounds. We have previously noted such interplay between the 5-OMe substituent and the influence of the 2,3,12,13-substituents on the MO energies and spectral characteristics of the bacteriochlorins.⁵⁷

D. Predictions of Redox Properties of Indium Bacteriochlorins. A prior study of two dozen zinc chlorins showed a good correlation between the measured oxidation potential and the HOMO energy, and also between the measured reduction potential and the LUMO energy.⁵⁸ It would be difficult to use those correlations to predict the exact change in redox potentials from the changes in orbital energies, but the trends should be reliable (i.e., whether a given compound in a set will be easier to oxidize or harder to reduce than another). On the basis of such considerations, the data in Table 3 suggest the following. The average HOMO energy of -4.65 eV for the indium bacteriochlorins compared to -4.52 eV for the free base analogues indicates that the indium chelates will be harder to oxidize. Similarly, the average LUMO energy of -2.66 eV for the indium bacteriochlorins versus -2.34 eV for the free base analogues indicates that the indium chelates will be easier to reduce. Such predictions are valuable in potential applications of the bacteriochlorins where redox processes are desired (or to be avoided). For example, the relative redox properties are important in the mechanisms (Type I versus II) for forming reactive oxygen species in photodynamic therapy, as has been shown for free base bacteriochlorins^{4–6} and for various metalloporphyrin species including indium chelates.^{43,44} Collectively, comparisons and correlations such as those given above between the molecular orbital characteristics, substituent and metal effects, optical properties, and redox potentials facilitate the design of bacteriochlorins for diverse applications.

EXPERIMENTAL SECTION

General Procedures. ¹H NMR (300 MHz) spectra and ¹³C NMR spectra (100 MHz) were collected at room temperature in CDCl₃ unless noted otherwise. Silica gel (40 μm average particle size) was used for column chromatography. All solvents were reagent grade and were used as received unless noted otherwise. Electrospray ionization mass spectrometry (ESI-MS) data are reported for the molecular ion or protonated molecular ion. Laser desorption mass spectrometry (LD-MS) was performed in the absence of a matrix.

Acid Survey. Each reaction was carried out in a conical microreaction vial containing 5 mM DHDPA-T and an amount of InX₃ corresponding to 50 mM (assuming complete dissolution) for a 4-mL reaction. Each reaction vial was equipped with a conical stir bar and fitted with a Teflon septum. Reactions were done on a 0.020 mmol scale of DHDPA-T. The vials and stir bars were dried in an oven (120 °C). A 5 mM stock solution of DHDPA-T was prepared in the desired concentration using the appropriate anhydrous solvent. Anhydrous solvents (CH₂Cl₂, CH₃CN) were reagent grade and were used as received.

The appropriate amount of neat solid InX₃ reagent was placed in a microreaction vial, under argon flow from an inverted glass funnel connected to an argon line. The acid was then treated with 4.00 mL of the previously prepared 5 mM solution of DHDPA-T. The reaction mixtures were stirred at room temperature for 16 h, at which point the reactions were checked by TLC and UV–vis spectroscopy. If bacteriochlorin formation was observed, the reaction mixture was neutralized by treatment with excess triethylamine and then concentrated. The bacteriochlorins were then separated by column chromatography [silica, CH₂Cl₂/hexanes (2:1→1:0), then CH₂Cl₂/ethyl acetate (99:1→4:1)]. The fractions containing bacteriochlorins were collected, concentrated, and the yield was determined spectroscopically ($\epsilon_{Q_y} = 97,000 \text{ M}^{-1} \text{ cm}^{-1}$ for **In-MeOBC-T**; $\epsilon_{Q_y} = 120,000 \text{ M}^{-1} \text{ cm}^{-1}$ for **Fb-MeOBC-T**). TDC-T was not isolated for the survey reactions. The results are reported in Table 1.

Reaction monitoring by TLC analysis entailed removal from the reaction vial of a 1 μL sample, which was spotted directly onto the TLC plate [silica, CH₂Cl₂]. TLC analysis gave information regarding the

consumption of starting material, formation of **Fb-MeOBC-T**, **TDC-T**, and **In-MeOBC-T**. **Fb-MeOBC-T** has the highest R_f value, followed by **TDC-T** and **In-MeOBC-T** (least to most polar, respectively). The intensity of the TLC spot attributed to the **TDC-T** was visually compared to those of **Fb-MeOBC-T** and **In-MeOBC-T**.

Reaction monitoring by absorption spectroscopic analysis entailed removal from the reaction vial of a 5 μL sample, which was diluted in 2.5 mL of $\text{CH}_2\text{Cl}_2/\text{EtOH}$ (3:1) in a UV-vis cuvette and checked for the presence of the characteristic bacteriochlorin Q_y absorption band (>700 nm). Then, one drop of triethylamine was added to the cuvette to neutralize any putative protonated bacteriochlorins, whereupon the absorption spectrum was measured again. When the total yield of bacteriochlorin was lower than $\sim 0.5\%$ (no prominent Q_y absorption >700 nm), the reaction mixture was not further analyzed.

In(III)Cl-5-methoxy-8,8,18,18-tetramethyl-2,12-bis(4-methylphenyl)bacteriochlorin (In-MeOBC-T). A solution of **DHDPA-T** (502 mg, 1.48 mmol) in CH_3CN (114 mL) was treated with InBr_3 (1.62 g, 4.57 mmol). The reaction mixture was stirred at room temperature for 16 h. Saturated aqueous NaHCO_3 was added, and the mixture was extracted with ethyl acetate. The organic layer was washed with brine, dried (Na_2SO_4), concentrated and chromatographed [silica, $\text{CH}_2\text{Cl}_2/\text{hexanes}$ (2:1)]. The first band (light green) was collected (**Fb-MeOBC-T**, 7.9 mg, 1.8%) and then the column was eluted with CH_2Cl_2 to afford the second band (dark green) (**TDC-T**, 16.7 mg, 3.7%). Further elution with ethyl acetate/ CH_2Cl_2 (1:4) afforded the third band (pink). The pink material was collected and again chromatographed [silica, ethyl acetate/hexanes (2:1)] to afford a pink solid (75 mg, 15%): $^1\text{H NMR } \delta$ 1.80 (s, 3H), 1.81 (s, 3H), 2.05 (s, 3H), 2.08 (s, 3H), 2.60 (s, 6H), 4.38 (d, $J = 16.8$ Hz, 1H), 4.44 (d, $J = 17.2$ Hz, 1H), 4.52 (d, $J = 17.2$ Hz, 1H), 4.52 (s, 3H), 4.59 (d, $J = 16.8$ Hz, 1H), 7.57 (d, $J = 8.0$ Hz, 4H), 8.02 (d, $J = 8.0$ Hz, 2H), 8.05 (d, $J = 8.0$ Hz, 2H), 8.66 (s, 1H), 8.71 (s, 1H), 8.75 (s, 1H), 8.78 (s, 1H), 8.99 (s, 1H); LD-MS obsd 728.0 (M+), obsd 693.0 (M - Cl); FAB-MS obsd 728.1799, calcd 728.1773 ($\text{C}_{39}\text{H}_{38}\text{ClInN}_4\text{O}$); ESI-MS obsd 693.2071, calcd 693.2079 [(M - Cl) $^+$, M = $\text{C}_{39}\text{H}_{38}\text{ClInN}_4\text{O}$]; λ_{abs} (toluene)/nm 355 ($\epsilon = 71,000 \text{ M}^{-1} \text{ cm}^{-1}$), 389 (69,000), 554 (21,000), 760 (97,000); λ_{em} (λ_{exc} 551 nm) = 768 nm. Elemental analysis (Anal. Calcd. for $\text{C}_{39}\text{H}_{38}\text{ClInN}_4\text{O}$: C, 64.25; H, 5.25; Cl, 4.86; N, 7.69. Found: C, 59.28; H, 5.13; Cl, 3.20; N, 6.33; Br, 0.0), while not in complete agreement with theory, showed the presence of chloride rather than bromide. The low value found for chloride (3.20 vs 4.96 expected) may stem from an admixture wherein hydroxide serves as apical ligand.

In(III)Cl-5-methoxy-8,8,18,18-tetramethylbacteriochlorin (In-MeOBC-H). A solution of **DHDPA-H** (673 mg, 2.71 mmol) in CH_3CN (200 mL) was treated with InBr_3 (2.96 g, 8.35 mmol). The reaction mixture was stirred at room temperature for 16 h. Saturated aqueous NaHCO_3 was added, and the mixture was extracted with ethyl acetate. The organic layer was washed with brine, dried (Na_2SO_4), concentrated and chromatographed [silica, $\text{CH}_2\text{Cl}_2/\text{MeOH}$ (9:1)] to afford a dark pink band (120 mg, 8.6%): LD-MS obsd 513.7, calcd 513.3 [(M - Cl) $^+$, M = $\text{C}_{25}\text{H}_{26}\text{ClInN}_4\text{O}$]; λ_{abs} (toluene) 351, 383, 550, 741 nm; λ_{em} (λ_{exc} 551 nm) = 746 nm. Anal. Calcd. for $\text{C}_{25}\text{H}_{26}\text{ClInN}_4\text{O}$: C, 54.72; H, 4.78; Cl, 6.46; N, 10.21. Found: C, 54.64; H, 5.07; Cl, 6.55; N, 8.44; Br, trace = <2.5).

3,13-Bis(ethoxycarbonyl)-2,8,8,12,18,18-hexamethylbacteriochlorin (Fb-HBC-MeEs), **In(III)Cl-3,13-bis(ethoxycarbonyl)-2,8,8,12,18,18-hexamethylbacteriochlorin (In-HBC-MeEs)**, **1H,22H,24H-7,8,17,18-tetradehydro-1-(1,1-dimethoxymethyl)-3,3,7,13,13,17-hexamethyl-8,18-bis(ethoxycarbonyl)-corrin (TDC-MeEs)**, and **In(III)Cl-3,13-bis(ethoxycarbonyl)-5-methoxy-2,8,8,12,18,18-hexamethylbacteriochlorin (In-MeOBC-MeEs)**. A solution of **DHDPA-MeEs** (549 mg, 1.64 mmol) in CH_3CN (126 mL) was treated with InBr_3 (1.79 g, 5.05 mmol). The reaction mixture was stirred at room temperature for 16 h. Saturated aqueous NaHCO_3 was added, and the mixture was extracted with

ethyl acetate. The organic layer was washed with brine, dried (Na_2SO_4), concentrated, and chromatographed [silica, $\text{CH}_2\text{Cl}_2/\text{ethyl acetate}$ (1:0 \rightarrow 5:1)]. The first band (light green) afforded **Fb-HBC-MeEs** (10.9 mg, 2.4%), the second band (light green) afforded **Fb-MeOBC-MeEs** (7.7 mg, 1.6%), the third band (dark green) afforded **TDC-MeEs** (55 mg, 11%), the fourth band (pink) afforded **In-HBC-MeEs** (5.5 mg, 1.0%), and the fifth band (pink) afforded **In-MeOBC-MeEs** (10.9 mg, 1.7%).

Fb-HBC-MeEs: $^1\text{H NMR } \delta$ -1.48 (brs, 2H), 1.69 (t, $J = 7.15$ Hz, 6H), 1.92 (s, 12H), 3.62 (s, 6H), 4.39 (s, 4H), 4.76 (q, $J = 7.15$ Hz, 4H), 8.61 (s, 2H), 9.63 (s, 2H); $^{13}\text{C NMR } \delta$ 13.6, 15.0, 31.3, 46.1, 52.1, 61.1, 94.8, 98.7, 134.3, 134.9, 135.6, 160.7, 166.9, 171.2; ESI-MS obsd 542.2880, calcd 542.2887 (M = $\text{C}_{32}\text{H}_{38}\text{N}_4\text{O}_4$); λ_{abs} (CH_2Cl_2) 353, 383, 518, 758 nm.

TDC-MeEs: $^1\text{H NMR } \delta$ 1.03 (s, 3H), 1.23 (s, 3H), 1.28 (s, 3H), 1.36-1.47 (m, 9H), 1.98 (d, $J = 14.03$ Hz, 1H), 2.34 (s, 3H), 2.39 (s, 3H), 2.57 (d, $J = 14.03$ Hz, 1H), 2.65, 2.71 (AB, $^2J = 18.8$ Hz, 2H), 3.09 (s, 3H), 3.44 (s, 3H), 4.22-4.45 (m, 4H), 4.89 (s, 1H), 5.54 (s, 1H), 5.77 (s, 1H), 6.27 (s, 1H), 11.03 (brs, 1H), 11.80 (brs, 1H); $^{13}\text{C NMR } \delta$ 11.6, 11.8, 14.5, 14.8, 25.8, 29.5, 29.9, 30.6, 40.4, 45.9, 49.7, 52.8, 57.3, 58.3, 59.4, 61.1, 80.7, 93.7, 95.7, 100.1, 108.7, 109.0, 116.7, 127.0, 127.1, 146.6, 147.1, 147.4, 149.0, 163.6, 163.9, 166.5, 171.3, 182.5; ESI-MS obsd 605.3330, calcd 605.3334 [(M + H) $^+$, M = $\text{C}_{34}\text{H}_{44}\text{N}_4\text{O}_6$]; λ_{abs} (CH_2Cl_2) 443, 620, 685 nm.

In-HBC-MeEs: $^1\text{H NMR } \delta$ 1.68 (t, $J = 7.15$ Hz, 6H), 1.88 (s, 6H), 2.09 (s, 6H), 3.58 (s, 6H), 4.42 (d, $J = 17.2$ Hz, 2H), 4.59 (d, $J = 17.2$ Hz, 2H), 4.74 (q, $J = 7.15$ Hz, 4H), 8.64 (s, 2H), 9.71 (s, 2H); ESI-MS obsd 655.1768, calcd 655.1770 [(M - Cl) $^+$, M = $\text{C}_{32}\text{H}_{36}\text{InClN}_4\text{O}_4$]; λ_{abs} (toluene) 351, 393, 554, 778 nm; λ_{em} (λ_{exc} 554 nm) = 787 nm.

In-MeOBC-MeEs: $^1\text{H NMR } \delta$ 1.60 (t, $J = 7.15$ Hz, 3H), 1.67 (t, $J = 7.15$ Hz, 3H), 1.82 (s, 3H), 1.84 (s, 3H), 2.07 (s, 3H), 2.12 (s, 3H), 3.31 (s, 3H), 3.58 (s, 3H), 4.26 (s, 3H), 4.38 (d, $J = 17.2$ Hz, 1H), 4.46 (s, 2H), 4.59 (d, $J = 17.2$ Hz, 1H), 4.74 (q, $J = 7.15$ Hz, 4H), 8.50 (s, 1H), 8.65 (s, 1H), 9.67 (s, 1H); ESI-MS obsd 685.1875, calcd 685.1876 [(M - Cl) $^+$, M = $\text{C}_{33}\text{H}_{38}\text{InClN}_4\text{O}_5$]; λ_{abs} (toluene) 358, 393, 563, 763 nm; λ_{em} (λ_{exc} 563 nm) = 768 nm.

Extinction Coefficients. The extinction coefficient of **In-MeOBC-T** was determined by dissolving a known quantity of the bacteriochlorin (~ 6 mg) in 100 mL of toluene. Then a known amount ($\sim 100 \mu\text{L}$) of this solution was added to a quartz cuvette containing 3.0 mL of toluene. The absorption spectrum was recorded at room temperature. The extinction coefficient of **In-MeOBC-T** determined and used herein for quantitative studies was $\epsilon = 97,000 \text{ M}^{-1} \text{ cm}^{-1}$ for the Q_y transition. The extinction coefficients for the Q_y transition of **Fb-HBC-T** and **Fb-MeOBC-T** are $130,000 \text{ M}^{-1} \text{ cm}^{-1}$ and $120,000 \text{ M}^{-1} \text{ cm}^{-1}$, respectively.³⁸

Photophysical Measurements. Static and time-resolved photophysical measurements were performed as described previously.⁴⁴ Measurement of the fluorescence (Φ_f) and triplet-excited-state (Φ_{isc}) quantum yields and singlet (τ_s) and triplet (τ_T) lifetimes utilized, unless noted otherwise, dilute (μM) Ar-purged toluene solutions at room temperature. Samples for Φ_f measurements had an absorbance <0.12 at the excitation wavelength. The Φ_f values were generally determined with respect to two standards and the results averaged. The standards were (1) free base meso-tetraphenylporphyrin (**FbTPP**) in nondegassed toluene, for which $\Phi_f = 0.070$ was established with respect to the zinc chelate **ZnTPP** in nondegassed toluene ($\Phi_f = 0.030$),⁵⁹ consistent with prior results on **FbTPP**,⁶⁰ and (2) 8,8,18,18-tetramethylbacteriochlorin²² in Ar-purged toluene, for which $\Phi_f = 0.14$ was established with respect to **FbTPP** and chlorophyll *a* (**Chl a**) in deoxygenated benzene⁶¹ or toluene⁶² ($\Phi_f = 0.325$).

The τ_s value for each indium bacteriochlorin was first probed using a time correlated single photon counting (TCSPC) instrument that employed Soret excitation flashes derived from a nitrogen-pumped dye laser (PTI LaserStrobe) and a Gaussian instrument response

function of 0.6 ns. These measurements indicated that the τ_S values were within the instrument response and likely in the range 0.2–0.4 ns. The lifetimes were then determined using ultrafast pump–probe absorption spectroscopy employing 130 fs excitation pulses in the Q_y band and probing from 440–660 nm. Global analysis of the data set yielded the reported values. The τ_S values for the free base bacteriochlorins were determined using the above-mentioned TCSPC apparatus as well as a fluorescence modulation technique (Spex Tau2);⁶³ the results from the two techniques were generally averaged.

The Φ_{isc} values were obtained using a transient-absorption technique in which the extent of bleaching of the ground-state $Q(1,0)$ band due to the lowest singlet excited state was measured immediately following a 130 fs flash in the $Q_x(0,0)$ or $Q_y(0,0)$ bands and compared with that due to the lowest triplet excited state at the asymptote of the singlet excited-state decay.⁴⁴ For the free base bacteriochlorins, the bleaching signals are referenced to a relatively featureless transient absorption, which are not substantially different for the S_1 and S_0 excited states. In the case of the indium chelates, the spectra are more featured and show larger differences between the two states. Thus, Gaussian fitting of the spectra (as well as more routine linear interpolation of the excited-state absorption across the ground-state bleaching region) was utilized to encompass a reasonable range of spectral shapes; an average value of the triplet yields obtained by these methods is reported for each bacteriochlorin.

Density Functional Theory Calculations. DFT calculations were performed with Spartan '08 for Windows version 1.2.0 in parallel mode⁶⁴ on a PC equipped with an Intel i7-975 CPU, 24 GB ram, and three 300 GB, 10 k rpm hard drives. The hybrid B3LYP functional and the LACVP basis set were employed. The equilibrium geometries were fully optimized using the default parameters of the Spartan '08 program.

■ ASSOCIATED CONTENT

S Supporting Information. Investigation of alternative reaction conditions for the formation of indium bacteriochlorins; identification of refined conditions for reaction of a dihydrodi-pyrrin-acetal in the presence of TMSOTf and 2,6-DTBP; and further experimental procedures. This material is available free of charge via the Internet at <http://pubs.acs.org>.

■ AUTHOR INFORMATION

Corresponding Author

*E-mail: david.bocian@ucr.edu (D.F.B.), holten@wustl.edu (D.H.), jlindsey@ncsu.edu (J.S.L.).

■ ACKNOWLEDGMENT

This work was supported by grants from the Division of Chemical Sciences, Geosciences and Biosciences Division, Office of Basic Energy Sciences of the U.S. Department of Energy to D.F.B. (DE-FG02-05ER15660), D.H. (DE-FG02-05ER15661), and J.S.L. (DE-FG02-96ER14632). R.M.D. and C.E.S. were supported by summer fellowships from the JimmyV Cancer Therapeutics Training Program at North Carolina State University. Mass spectra were obtained at the Mass Spectrometry Laboratory for Biotechnology at North Carolina State University. Partial funding for the Facility was obtained from the North Carolina Biotechnology Center and the National Science Foundation.

■ REFERENCES

(1) Scheer, H. In *Chlorophylls and Bacteriochlorophylls. Biochemistry, Biophysics, Functions and Applications*; Grimm, B., Porra, R. J., Rüdiger, W., Scheer, H., Eds.; Springer: Dordrecht, The Netherlands, 2006; Advances in Photosynthesis and Respiration, Vol. 25, pp 1–26.

(2) Kobayashi, M.; Akiyama, M.; Kano, H.; Kise, H. In *Chlorophylls and Bacteriochlorophylls. Biochemistry, Biophysics, Functions and Applications*; Grimm, B., Porra, R. J., Rüdiger, W., Scheer, H., Eds.; Springer: Dordrecht, The Netherlands, 2006; pp 79–94.

(3) Ethirajan, M.; Chen, Y.; Joshi, P.; Pandey, R. K. *Chem. Soc. Rev.* **2011**, *40*, 340–362.

(4) Mroz, P.; Huang, Y.-Y.; Szokalska, A.; Zhiyentayev, T.; Janjua, S.; Nifli, A.-P.; Sherwood, M. E.; Ruzi , C.; Borbas, K. E.; Fan, D.; Krayner, M.; Balasubramanian, T.; Yang, E.; Kee, H. L.; Kirmaier, C.; Diers, J. R.; Bocian, D. F.; Holten, D.; Lindsey, J. S.; Hamblin, M. R. *FASEB J.* **2010**, *24*, 3160–3170.

(5) Huang, Y.-Y.; Mroz, P.; Zhiyentayev, T.; Sharma, S. K.; Balasubramanian, T.; Ruzi , C.; Krayner, M.; Fan, D.; Borbas, K. E.; Yang, E.; Kee, H. L.; Kirmaier, C.; Diers, J. R.; Bocian, D. F.; Holten, D.; Lindsey, J. S.; Hamblin, M. R. *J. Med. Chem.* **2010**, *53*, 4018–4027.

(6) Huang, L.; Huang, Y.-Y.; Mroz, P.; Tegos, G. P.; Zhiyentayev, T.; Sharma, S. K.; Lu, Z.; Balasubramanian, T.; Krayner, M.; Ruzi , C.; Yang, E.; Kee, H. L.; Kirmaier, C.; Diers, J. R.; Bocian, D. F.; Holten, D.; Lindsey, J. S.; Hamblin, M. R. *Antimicrob. Agents Chemother.* **2010**, *54*, 3834–3841.

(7) O'Connor, A. E.; Gallagher, W. M.; Byrne, A. T. *Photochem. Photobiol.* **2009**, *85*, 1053–1074.

(8) Grin, M. A.; Mironov, A. F.; Shtil, A. A. *Anti-Cancer Agents Med. Chem.* **2008**, *8*, 683–697.

(9) Brandis, A. S.; Salomon, Y.; Scherz, A. In *Chlorophylls and Bacteriochlorophylls. Biochemistry, Biophysics, Functions and Applications*; Grimm, B., Porra, R. J., Rüdiger, W., Scheer, H., Eds.; Springer: Dordrecht, The Netherlands, 2006; pp 485–494.

(10) Nyman, E. S.; Hynninen, P. H. *J. Photochem. Photobiol., B* **2004**, *73*, 1–28.

(11) Chen, Y.; Li, G.; Pandey, R. K. *Curr. Org. Chem.* **2004**, *8*, 1105–1134.

(12) Bonnett, R. *Chemical Aspects of Photodynamic Therapy*; Gordon and Breach Science Publishers: Amsterdam, The Netherlands, 2000.

(13) Singh, S.; Aggarwal, A.; Thompson, S.; Tom , J. P. C.; Zhu, X.; Samaroo, D.; Vinodu, M.; Gao, R.; Drain, C. M. *Bioconjugate Chem.* **2010**, *21*, 2136–2146.

(14) Kee, H. L.; Diers, J. R.; Ptaszek, M.; Muthiah, C.; Fan, D.; Lindsey, J. S.; Bocian, D. F.; Holten, D. *Photochem. Photobiol.* **2009**, *85*, 909–920.

(15) Kee, H. L.; Nothdurft, R.; Muthiah, C.; Diers, J. R.; Fan, D.; Ptaszek, M.; Bocian, D. F.; Lindsey, J. S.; Culver, J. P.; Holten, D. *Photochem. Photobiol.* **2008**, *84*, 1061–1072.

(16) Akers, W.; Lesage, F.; Holten, D.; Achilefu, S. *Mol. Imaging* **2007**, *6*, 237–246.

(17) Frangioni, J. V. *Curr. Opin. Chem. Biol.* **2003**, *7*, 626–634.

(18) Licha, K. *Top. Curr. Chem.* **2002**, *222*, 1–29.

(19) Sutton, J. M.; Clarke, O. J.; Fernandez, N.; Boyle, R. W. *Bioconjugate Chem.* **2002**, *13*, 249–263.

(20) (a) De Rosa, S. C.; Brenchley, J. M.; Roederer, M. *Nat. Med.* **2003**, *9*, 112–117. (b) Perfetto, S. P.; Chattopadhyay, P. K.; Roederer, M. *Nat. Rev. Immunol.* **2004**, *4*, 648–655.

(21) Lindsey, J. S.; Mass, O.; Chen, C.-Y. *New J. Chem.* **2011**, *35*, 511–516.

(22) Taniguchi, M.; Cramer, D. L.; Bhise, A. D.; Kee, H. L.; Bocian, D. F.; Holten, D.; Lindsey, J. S. *New J. Chem.* **2008**, *32*, 947–958.

(23) Stromberg, J. R.; Marton, A.; Kee, H. L.; Kirmaier, C.; Diers, J. R.; Muthiah, C.; Taniguchi, M.; Lindsey, J. S.; Bocian, D. F.; Meyer, G. J.; Holten, D. *J. Phys. Chem. C* **2007**, *111*, 15464–15478.

(24) (a) Weersink, R. A.; Forbes, J.; Bisland, S.; Trachtenberg, J.; Elhilali, M.; Br n, P. H.; Wilson, B. C. *Photochem. Photobiol.* **2005**, *81*, 106–113. (b) Koudinova, N. V.; Pinthus, J. H.; Brandis, A.; Brenner, O.; Bendel, P.; Ramon, J.; Eshhar, Z.; Scherz, A.; Salomon, Y. *Int. J. Cancer* **2003**, *104*, 782–789. (c) Chen, Q.; Huang, Z.; Luck, D.; Beckers, J.; Brun, P.-H.; Wilson, B. C.; Scherz, A.; Salomon, Y.; Hetzel, F. W. *Photochem. Photobiol.* **2002**, *76*, 438–445.

- (25) Vokrat-Haglilil, Y.; Weiner, L.; Brumfeld, V.; Brandis, A.; Salomon, Y.; McIlroy, B.; Wilson, B. C.; Pawlak, A.; Rozanowska, M.; Sarna, T.; Scherz, A. *J. Am. Chem. Soc.* **2005**, *127*, 6487–6497.
- (26) (a) Brandis, A.; Mazor, O.; Neumark, E.; Rosenbach-Belkin, V.; Salomon, Y.; Scherz, A. *Photochem. Photobiol.* **2005**, *81*, 983–993. (b) Mazor, O.; Brandis, A.; Plaks, V.; Neumark, E.; Rosenbach-Belkin, V.; Salomon, Y.; Scherz, A. *Photochem. Photobiol.* **2005**, *81*, 342–351.
- (27) (a) Ashur, L.; Goldschmidt, R.; Pinkas, I.; Salomon, Y.; Szweczyk, G.; Sarna, T.; Scherz, A. *J. Phys. Chem. A* **2009**, *113*, 8027–8037. (b) Kozyrev, A. N.; Chen, Y.; Goswami, L. N.; Tabaczynski, W. A.; Pandey, R. K. *J. Org. Chem.* **2006**, *71*, 1949–1960. (c) Limantara, L.; Koehler, P.; Wilhelm, B.; Porra, R. J.; Scheer, H. *Photochem. Photobiol.* **2006**, *82*, 770–780. (d) Fiedor, J.; Fiedor, L.; Kammhuber, N.; Scherz, A.; Scheer, H. *Photochem. Photobiol.* **2002**, *76*, 145–152.
- (28) Hartwich, G.; Fiedor, L.; Simonin, I.; Cmiel, E.; Schäfer, W.; Noy, D.; Scherz, A.; Scheer, H. *J. Am. Chem. Soc.* **1998**, *120*, 3675–3683.
- (29) Wasielewski, M. R. *Tetrahedron Lett.* **1977**, *18*, 1373–1376.
- (30) (a) Fukuzumi, S.; Ohkubo, K.; Zheng, X.; Chen, Y.; Pandey, R. K.; Zhan, R.; Kadish, K. M. *J. Phys. Chem. B* **2008**, *112*, 2738–2746. (b) Kunieda, M.; Tamiaki, H. *J. Org. Chem.* **2005**, *70*, 820–828. (c) Donohoe, R. J.; Frank, H. A.; Bocian, D. F. *Photochem. Photobiol.* **1988**, *48*, 531–537. (d) Schneider, E. *J. Am. Chem. Soc.* **1941**, *63*, 1477–1478.
- (31) (a) Musewald, C.; Hartwich, G.; Lossau, H.; Gilch, P.; Pöllinger-Dammer, F.; Scheer, H.; Michel-Beyerle, M. E. *J. Phys. Chem. B* **1999**, *103*, 7055–7060. (b) Musewald, C.; Hartwich, G.; Pöllinger-Dammer, F.; Lossau, H.; Scheer, H.; Michel-Beyerle, M. E. *J. Phys. Chem. B* **1998**, *102*, 8336–8342. (c) Teuchner, K.; Stiel, H.; Leupold, D.; Scherz, A.; Noy, D.; Simonin, I.; Hartwich, G.; Scheer, H. *J. Lumin.* **1997**, *72–74*, 612–614.
- (32) Vasudevan, J.; Stibrany, R. T.; Bumby, J.; Knapp, S.; Potenza, J. A.; Emge, T. J.; Schugar, H. J. *J. Am. Chem. Soc.* **1996**, *118*, 11676–11677.
- (33) Barkigia, K. M.; Miura, M.; Thompson, M. A.; Fajer, J. *Inorg. Chem.* **1991**, *30*, 2233–2236.
- (34) Donohoe, R. J.; Atamian, M.; Bocian, D. F. *J. Phys. Chem.* **1989**, *93*, 2244–2252.
- (35) Fajer, J.; Borg, D. C.; Forman, A.; Felton, R. H.; Dolphin, D.; Vegh, L. *Proc. Natl. Acad. Sci. U.S.A.* **1974**, *71*, 994–998.
- (36) Hu, S.; Mukherjee, A.; Spiro, T. G. *J. Am. Chem. Soc.* **1993**, *115*, 12366–12377.
- (37) Ruzié, C.; Krayer, M.; Balasubramanian, T.; Lindsey, J. S. *J. Org. Chem.* **2008**, *73*, 5806–5820.
- (38) Kim, H.-J.; Lindsey, J. S. *J. Org. Chem.* **2005**, *70*, 5475–5486.
- (39) Krayer, M.; Ptaszek, M.; Kim, H.-J.; Meneely, K. R.; Fan, D.; Secor, K.; Lindsey, J. S. *J. Org. Chem.* **2010**, *75*, 1016–1039.
- (40) Aravindu, K.; Krayer, M.; Kim, H.-J.; Lindsey, J. S. *New J. Chem.* **2011**, *35*, DOI:10.1039/C1NJ20027E.
- (41) Buchler, J. W.; Schneehage, H. H. *Tetrahedron Lett.* **1972**, *36*, 3803–3806.
- (42) (a) Rosenfeld, A.; Morgan, J.; Goswami, L. N.; Ohulchanskyy, T.; Zheng, X.; Prasad, P. N.; Oseroff, A.; Pandey, R. K. *Photochem. Photobiol.* **2006**, *82*, 626–634. (b) Dolmans, D. E. J. G. J.; Kadambi, A.; Hill, J. S.; Waters, C. A.; Robinson, B. C.; Walker, J. P.; Fukumura, D.; Jain, R. K. *Cancer Res.* **2002**, *62*, 2151–2156. (c) Robinson, B. C.; Phadke, A. S. U.S. Patent 6,444,194 B1, 2002.
- (43) Mroz, P.; Bhaumik, J.; Dogutan, D. K.; Aly, Z.; Kamal, Z.; Khalid, L.; Kee, H. L.; Bocian, D. F.; Holten, D.; Lindsey, J. S.; Hamblin, M. R. *Cancer Lett.* **2009**, *282*, 63–76.
- (44) Kee, H. L.; Bhaumik, J.; Diers, J. R.; Mroz, P.; Hamblin, M. R.; Bocian, D. F.; Lindsey, J. S.; Holten, D. *J. Photochem. Photobiol. A: Chem.* **2008**, *200*, 346–355.
- (45) Da Silva, A. R.; Pelegrino, A. C.; Tedesco, A. C.; Jorge, R. A. *J. Braz. Chem. Soc.* **2008**, *19*, 491–501.
- (46) Dogutan, D. K.; Zaidi, S. H. H.; Thamyongkit, P.; Lindsey, J. S. *J. Org. Chem.* **2007**, *72*, 7701–7714.
- (47) Takagi, S.; Kato, Y.; Furuta, H.; Onaka, S.; Miyamoto, T. K. *J. Organomet. Chem.* **1992**, *429*, 287–299.
- (48) Cornillion, J.-L.; Anderson, J. E.; Kadish, K. M. *Inorg. Chem.* **1986**, *25*, 991–995.
- (49) (a) Lin, S.-J.; Hong, T.-N.; Tung, J.-Y.; Chen, J.-H. *Inorg. Chem.* **1997**, *36*, 3886–3891. (b) Lee, Y.-Y.; Chen, J.-H.; Hsieh, H.-Y. *Polyhedron* **2003**, *22*, 1633–1639.
- (50) Taft, C. D.; Holten, D. *Photobiochem. Photobiophys.* **1983**, *6*, 201–209.
- (51) Holten, D.; Gouterman, M.; Parson, W. W.; Windsor, M. W.; Rockley, M. G. *Photochem. Photobiol.* **1976**, *23*, 415–423.
- (52) Birks, J. B. *Photophysics of Aromatic Molecules*; Wiley-Interscience: London, 1970; pp 140–192.
- (53) (a) Gentemann, S.; Medforth, C. J.; Ema, T.; Nelson, N. Y.; Smith, K. M.; Fajer, J.; Holten, D. *Chem. Phys. Lett.* **1995**, *245*, 441–447. (b) Gentemann, S.; Nelson, N. Y.; Jaquinod, L.; Nurco, D. J.; Leung, S. H.; Medforth, C. J.; Smith, K. M.; Fajer, J.; Holten, D. *J. Phys. Chem. B* **1997**, *101*, 1247–1254. (c) Retsek, J. L.; Medforth, C. J.; Nurco, D. J.; Gentemann, S.; Chirvony, V. S.; Smith, K. M.; Holten, D. *J. Phys. Chem. B* **2001**, *105*, 6396–6411.
- (54) (a) Linnanto, J.; Korppi-Tommola, J. *Phys. Chem. Chem. Phys.* **2006**, *8*, 663–687. (b) Petit, L.; Quartarolo, A.; Adamo, C.; Russo, N. *J. Phys. Chem. B* **2006**, *110*, 2398–2404.
- (55) (a) Petke, J. D.; Maggiora, G. M.; Shipman, L. L.; Christoffersen, R. E. *Photochem. Photobiol.* **1980**, *32*, 399–414. (b) Weiss, C., Jr. *J. Mol. Spectrosc.* **1972**, *44*, 37–80.
- (56) (a) Gouterman, M. In *The Porphyrins*; Dolphin, D., Ed.; Academic Press: New York, 1978; Vol. 3, pp 1–165. (b) Gouterman, M. *J. Mol. Spectrosc.* **1961**, *6*, 138–163.
- (57) Krayer, M.; Yang, E.; Diers, J. R.; Bocian, D. F.; Holten, D.; Lindsey, J. S. *New J. Chem.* **2011**, *35*, 587–601.
- (58) Kee, H. L.; Kirmaier, C.; Tang, Q.; Diers, J. R.; Muthiah, C.; Taniguchi, M.; Laha, J. K.; Ptaszek, M.; Lindsey, J. S.; Bocian, D. F.; Holten, D. *Photochem. Photobiol.* **2007**, *83*, 1125–1143.
- (59) Seybold, P. G.; Gouterman, M. *J. Mol. Spectrosc.* **1969**, *31*, 1–13.
- (60) Gradyushko, A. T.; Sevchenko, A. N.; Solovoyov, K. N.; Tsvirko, M. P. *Photochem. Photobiol.* **1970**, *11*, 387–400.
- (61) Weber, G.; Teale, F. W. J. *Trans. Faraday Soc.* **1957**, *53*, 646–655.
- (62) Mass, O.; Taniguchi, M.; Ptaszek, M.; Springer, J. W.; Faries, K. M.; Diers, J. R.; Bocian, D. F.; Holten, D.; Lindsey, J. S. *New J. Chem.* **2011**, *35*, 76–88.
- (63) Kee, H. L.; Kirmaier, C.; Yu, L.; Thamyongkit, P.; Youngblood, W. J.; Calder, M. E.; Ramos, L.; Noll, B. C.; Bocian, D. F.; Scheidt, W. R.; Birge, R. R.; Lindsey, J. S.; Holten, D. *J. Phys. Chem. B* **2005**, *109*, 20433–20443.
- (64) Except for molecular mechanics and semi-empirical models, the calculation methods used in Spartan have been documented in: Shao, Y.; Molnar, L. F.; Jung, Y.; Kussmann, J.; Ochsenfeld, C.; Brown, S. T.; Gilbert, A. T. B.; Slipchenko, L. V.; Levchenko, S. V.; O'Neill, D. P.; DiStasio, R. A., Jr.; Lochan, R. C.; Wang, T.; Beran, G. J. O.; Besley, N. A.; Herbert, J. M.; Lin, C. Y.; Van Voorhis, T.; Chien, S. H.; Sodt, A.; Steele, R. P.; Rassolov, V. A.; Maslen, P. E.; Korambath, P. P.; Adamson, R. D.; Austin, B.; Baker, J.; Byrd, E. F. C.; Dachsel, H.; Doerksen, R. J.; Dreuw, A.; Dunietz, B. D.; Dutoi, A. D.; Furlani, T. R.; Gwaltney, S. R.; Heyden, A.; Hirata, S.; Hsu, C.-P.; Kedziora, G.; Khalliulin, R. Z.; Klunzinger, P.; Lee, A. M.; Lee, M. S.; Liang, W.-Z.; Lotan, I.; Nair, N.; Peters, B.; Proynov, E. I.; Pieniazek, P. A.; Rhee, Y. M.; Ritchie, J.; Rosta, E.; Sherrill, C. D.; Simmonett, A. C.; Subotnik, J. E.; Woodcock, H. L., III; Zhang, W.; Bell, A. T.; Chakraborty, A. K.; Chipman, D. M.; Keil, F. J.; Warshel, A.; Hehre, W. J.; Schaefer, H. F., III; Kong, J.; Krylov, A. I.; Gill, P. M. W.; Head-Gordon, M. *Phys. Chem. Chem. Phys.* **2006**, *8*, 3172–3191.